A lattice Boltzmann study of the non-Newtonian blood flow in stented aneurysm

Yong Hyun Kim, Sam Farhat, Xiafeng Xu, Joon Sang Lee

Department of Mechanical Engineering
Wayne State University
Detroit, MI, 48202, USA

ABSTRACT

The analysis of a flow pattern in cerebral aneurysms and the effect of strut shapes and stent porosity in 2D and 3D model are presented in this paper. The efficiency of a stent is related to several parameters, including porosity and stent strut shapes. The goal of this paper is to identify numerically how the stent strut shape and the porosity affect the hemodynamics properties of the flow inside an aneurysm. The lattice Boltzmann method (LBM) of a non-Newtonian blood fluid is used. To ease the code development, a scientific programming strategy based on object-oriented concepts is developed. An extrapolation method for wall and stent boundary conditions is used to resolve the characteristics of a highly complex flow. The reduced velocity, vorticity magnitude, and shear rate were observed when the proposed stent shapes and porosities are used. The rectangular strut shape stent is observed to be optimal and decrease the magnitude of the velocity by 89.25% in 2D model and 53.92% in 3D model in the aneurysm sac. Our results show how the porosity and stent strut shapes play a role and help us to understand the characteristics of stent strut design.

Key words: lattice Boltzmann method, extrapolation method, strut shape, porosity,

INTRODUCTION

Studies of aneurysm models have shown complex hemodynamic changes in an aneurysm after the placement of a stent across the aneurysm neck [1-3]. The hemodynamic properties of the blood inside an aneurysm are of great importance in the case of aneurysms by stents. Recently, stents have been used in minimal invasive treatments of aneurysms, as an alternative to by-pass surgery. Due to its limited permeability, the stent modifies the blood flow in the aneurysm. It is thought that the resulting flow stagnation promotes the formation of a stable thrombus in the aneurysm sac leading to its permanent occlusion. Therefore, the stent should modify the blood circulation in the aneurysm but not stop it. In particular, the optimal design of the stent structure is not studied with a function of strut shape of the stent in an aneurysm.

The flow over obstacles of different shapes and sizes has been studied due to its importance to engineering applications. Enhanced surfaces significantly alter the structure of the flow. It was found that shape and size of the rib affected the friction factor significantly [4].

Several experimental and numerical studies have been reported [2, 5 ,6]. The existence of large coherent vortex structures in lateral aneurysm model is emphasized. However, they do not discuss well the reduced flow mechanism by stents.

The main goal of this paper was to propose the effect of stent porosity and the effect of strut shape stent with a non-Newtonian extension to the standard LB model that incorporates correct blood rheology in case of small shear rate. This study was organized as follows. In the 2D model with ghost cell extrapolation method, the effects of stent porosity cases were studied with the steady flow condition. The second was that the effects of various strut shapes of stents were considered and analyzed by the flow reduction/enhancement in an aneurysm sac with the pulsatile flow condition in 2D model. In 3D model with bounce-back method, the flow characteristics were analyzed with or without a stent. In 2D and 3D models, averaged flow characteristics and shear rate with non-Newtonian fluid for the aneurysm were considered.

NUMERICAL METHOD

A. The lattice Boltzmann method

The LBM used in this study is the incompressible lattice Bhatnagar-Gross-Krook (BGK) model (D2Q9) [7] and the incompressible lattice BGK model (D3Q19) [8].

An incompressible viscous fluid is assumed in the present study. For a non-Newtonian fluid, effective viscosity μ is found to vary with local shear rate $\dot{\gamma}$. Carreau Model [9] was used in this study.

B. Boundary Conditions

In this study, two boundary methods for walls were used. The bounce-back method for 3D simulation was easy for implementation and supported the idea that LBM was ideal for simulating fluid flows in complicated geometries. But this method is only the first order in numerical accuracy at boundaries [10] unless the boundary is at the center between lattice nodes.

The extrapolation scheme for 2D simulation is of the second-order accuracy, and it is consistent with the accuracy of the D2Q9 model [11].

Results

A. Validation

Simulation capability to a variety of configurations with respect to the type of flow conditions to obtain a comprehensive comparison with analytical data was conducted.

The first validation test of the 2D extrapolation method of LBM was presented. The aneurysm model in this study was compared with the numerical study in Hirabayasi et al [12]. The velocity magnitude was compared at the aneurysm neck and the difference was less than 8% in 95.51% of porosity case.

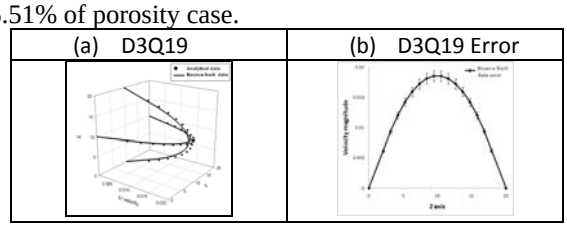

Figure 1. (a) velocity comparison in D3Q19, and (b) the error of velocity in D3Q19 model

The second validation of the fully developed flow in 3D model was shown in Fig. 1(a). The fully-developed channel flow driven by a constant pressure gradient was shown in Fig. 6(b). The profile of the analytical velocity (u_e) [13] is expressed as parabolic. $u_e = -\frac{R^2}{4\rho\nu}\frac{dp}{dx}\left[1-\left(\frac{r}{R}\right)^2\right]$, where the non-dimensional values of pressure gradient, $dp/dx = 2.026\times10^{-5}$, kinematic viscosity, $\nu = 0.026$, density, $\rho = 1$, and R is the radius of the channel, respectively. The Reynolds number of the flow was 30. The $20\times20\times80$ ($x\times y\times z$) lattices were used. The profiles of the velocity showed that the lattice Boltzmann solutions matched the analytical solutions within a 4.7 percent as shown in Fig. 1(a) and (b).

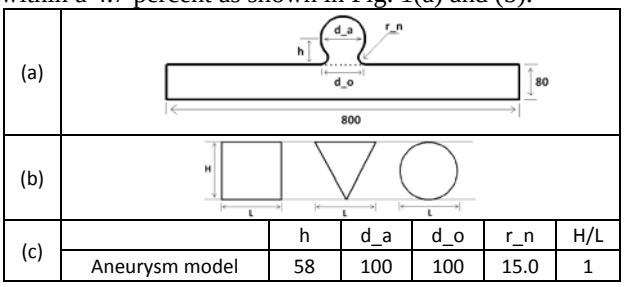

	h	d_a	d_o	r_n	H/L
Aneurysm model	58	100	100	15.0	1

Figure 2. (a) 2D aneurysm model , (b) strut shapes, and (c) aneurysm parameter

B. Flow patterns and vortex

The computational domain for D2Q9 model was shown in Fig. 2. In the cerebral artery, the Reynolds number within the aneurysm is less or about 30 [2] and the velocity magnitude is low (1cm/s). The relaxation time, $\tau = 0.58$, was chosen to produce a constant kinetic viscosity, $\nu = 0.026$, for infinite shear viscosity. The average density of the system was $\rho = 1.0$. The simulation size was 800×188 lattice sites, with a channel width made of 80 sites.

For unsteady flow, at the entry of the artery, the pulsatile inlet velocity as shown in Fig. 3 was used. The parabolic velocity profile at inlet was used. The maximum Reynolds number, used in this study was 20 based on the center velocity, 0.0065m/s, at t=0.3s (peak time). One million time steps were used in one pulsatile period and the time step, Δt, was $10^{-6}s$.

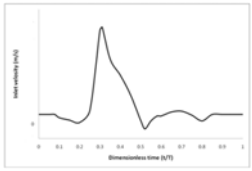

Figure 3, Inlet pulsatile profile

The geometric dimensions of struts were shown in Fig. 2(b). The ratio (H/L) of stents is 1, where H is the height of strut and L is the width of strut. The no-slip boundary condition on the stent surface was used as for the wall.

For this study, we consider 4 cases of unsteady condition in each strut shape and 4 cases of steady state conditions. These cases included three different strut shapes in Fig. 2(b) and four different porosity cases for each strut shape as shown in Table 1.

Table 1, Porosity cases

Case	Porosity (%)	Pore size
Case 1	95.51	35
Case 2	89.53	15
Case 3	83.59	11
Case 4	77.78	9

The Hemodynamic effects of stent implantation on a saccular aneurysm, its flow reduction to the aneurysm sac and critical non-Newtonian flow properties with respect to the strut shape and the stent porosity were studied.

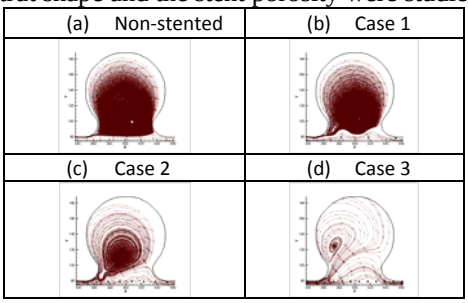

Figure 4, Streamline plot of the flow inside aneurysm with different porosity cases

To understand the effect of stents on the flow characteristics, mean velocity reduction, is defined as $\bar{v}_r = (\bar{v}^{ns} - \bar{v}^{st})/\bar{v}^{ns}\times100$,where $\bar{v}^{ns}$ and $\bar{v}^{st}$ are the averaged non-stented velocity and the averaged stented velocity in the aneurysm sac, respectively [12]. For more analysis, the mean velocity reduction can be replaced to the mean vorticity reduction, $\bar{\omega}_r$ and mean shear rate reduction rate, $\bar{\dot{\gamma}}_r$.

Another effect of the stent is introduced in this study and the so-called mean viscosity increase rate defined as $\bar{\mu}_c = (\bar{\mu}^{st} - \bar{\mu}^{ns})/\bar{\mu}^{st}\times100$, where $\bar{\mu}^{ns}$ and $\bar{\mu}^{st}$ are the averaged non-stented viscosity and the averaged stented viscosity in the aneurysm sac.

The Effect of Porosity

NSTI-Nanotech 2008, www.nsti.org, ISBN 978-1-4200-8505-1 Vol. 3

Fig. 4 showed the variation of the flow patterns in the stented aneurysm of a circular strut shape with the steady flow condition. In Fig. 4(a), the vortex in the non-stented aneurysm was driven directly by the flow in the parent vessel and was rather important. On the other hand, in Fig. 4(b), (c) and (d), the vortex was reduced with the stent.

In Table2, it was observed that small velocity magnitudes in the low porosity case compared with all other cases. The mean velocity was decreased by up to 86.8% in the case 3.

Fig. 4 and Table 2 suggested that this reduction was related to the stent porosity. The numerical results of Hirabayashi et al [12], using different stent porosity in various aneurysm sizes, showed that the low stent porosity was better for velocity reduction compared to the high porosity case.

Table 2, velocity reduction at the aneurysm neck

Strut shape	Porosity	$\bar{V}_r$	Umax
Circular shape	C1	46.3	0.016591
	C2	82.0	0.005897
	C3	86.8	0.004007
Without stent		0	0.025305

Stent porosity model can be occluded easily because of the large number of stent struts and the small velocity at the aneurysm neck. The numerical simulation [12] with LBM showed that the stent porosity alone was not sufficient to characterize uniquely the flow reduction in the aneurysm.

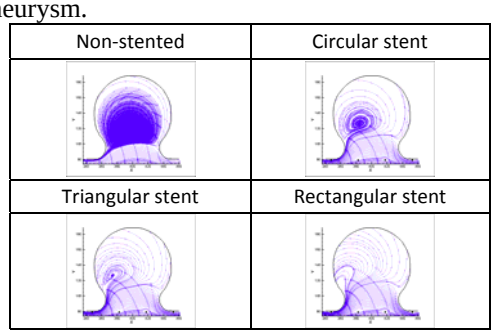

Figure 5, Streamline plot of the flow inside aneurysm with different strut shape stent

The Effect of Stent strut shapes

Different flow patterns in an aneurysm sac with different stent strut shapes were shown in Figs. 5 and 6. Figs. 5 and 6 showed that the velocity was significantly reduced and affected not only in the low porosity cases but also in various strut shape stents. The vortex was significantly reduced in the aneurysm sac in all strut shape stents Fig. 5 showed that the vortex was more reduced in the rectangular strut shape stents than in the other shape stents.

The u-velocity magnitudes were shown in Fig. 6. Since the u-velocity magnitude was higher than the v-velocity magnitude, the u-velocity magnitudes were analyzed in this study. It showed that the maximum velocity of the rectangular strut shape stent was reduced up to 25.9% compared with circular shape and 89% compared with non-stented model as shown in Fig. 6.

The mean flow characteristics reduction or enhancement rate at t=0.3s was shown in Fig. 7. It was observed that the rectangular strut shape stents was very effective to reduce flow into an aneurysm sac more than other strut shapes. The mean velocity reduction rate of the rectangular strut shape stent was up to 92% in case 4(Fig. 7(a)). By the reduced velocity, it was observed that the highest viscosity enhancement rate in the rectangular strut shape stents occurs (Fig. 7(b)). The width of rectangular strut shape stent was observed to be more effective on velocity reduction inside the aneurysm sac than the other stent strut shapes, Because the longer boundary layer in the rectangular strut shape stent was created along the parent artery and keeps the flow from moving into the aneurysm sac.

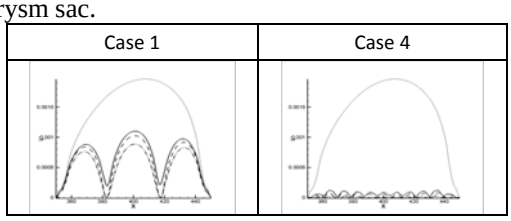

Figure 6, U-velocity magnitude in an aneurysm neck. (Rigid - circular, Dash - triangular, and Double dot - rectangular shape)

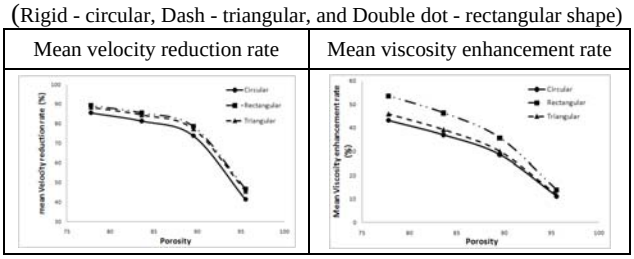

Figure 7, Mean values inside an aneruysm

3D aneurysm model

In this simulation, the 3D aneurysm model with a bounce-back boundary method was considered as shown in Fig. 8. In order to obtain the appropriate Reynolds number, $\mathrm{Re} = 75$, for the parent vessel flow. The relaxation time ($\tau = 0.58$) was chosen to produce a constant kinetic viscosity ($v = 0.026$) for infinite shear viscosity. The average density of the system was $\rho = 1.0$. The non-Newtonian fluid was used.

The constant pressure gradient $dp/dx \cong 4.17e-6$ is used rather than a pulsatile flow in order to simplify the study of flow reduction by stents. For the inlet and outlet, we used periodic boundaries.

In this study, the 2d aneurysm simulation showed that the rectangular strut shape stent was more effective than other shape stents. Therefore, in the 3D aneurysm model (84.9% porosity), the flow characteristics were compared with rectangular strut shape stent with non-stented model.

Velocity was compared with a non-stented aneurysm model (Fig. 9). Velocity was measured on A-A' (along with the parent vessel) and B-B' sections (across the parent vessel) in an aneurysm neck (Fig. 9). The velocity in an aneurysm neck was observed that stented model had

lower velocity, up to 85% reduction on A-A' section and up to 76.20% on B-B' section. The velocity iso-surface explained that flow into an aneurysm sac was prevented by the stent in Fig. 9.

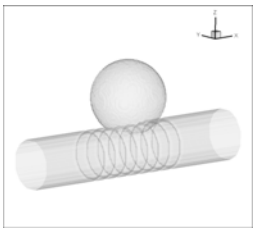

Aneurysm diameter	60
Parent vessel diameter	40
Porosity	84.98 %
Stent strut diameter	2
H/L	1
Re	75
dp/dx	4.17e-6
$200 \times 60 \times 96$ lattice	

Figure 8, 3D aneurysm geometry

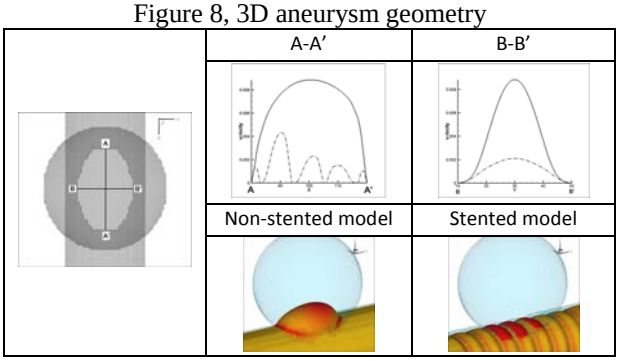

Figure 9, Comparison of velocity magnitude and velocity iso-surface

Table 3, Measured parameters in the 3D simulation

	$\bar{V}_r$	$\bar{\omega}_r$	$\bar{\mu}_r$
Non-stented	2.485e-4	5.198e-5	4.749e-3
Rectangular stent	1.145e-4	1.951e-5	5.522e-3

In Table 3, this velocity reduction affected the other flow characteristics, e.g. vorticity, and visocisty, in the aneurysm sac. It was observed that shear rate was reduced on a stented aneurysm as well as vorticity.

Fig. 10 (a) showed the variation of the flow patterns in non-stented and stented aneurysms. The vortex was reduced with a stent. The secondary flow was also reduced in stented aneurysm. A low secondary flow region had a high viscosity and was related to the low vorticity region [14]. The viscosity in the aneurysm sac was increased with reduced flow by the stent as shown in Fig. 10 (b).

Discussion

A fluid solver based on a lattice Boltzmann method (LBM) is developed and used in 2D and 3D numerical simulations. The flow in aneurysms with different porosity and different shape stents is demonstrated to examine the flow inside the aneurysm. Three shapes of stents and four different porosity cases were investigated in a 2D aneurysm model and the rectangular strut shape was used in a 3D aneurysm model.

The reduced flow and smaller mean velocity magnitude in the aneurysm sac were observed when the low porosity case used. With lower porosity, the velocity was reduced by up to 86.8% with a circular strut shape stent. However, the stent porosity is not enough to describe the effect of the stent alone.

The strut shape, as well as porosity, was to describe the effect of the stent on the velocity reduction and shear rate reduction. So they must be taken into account to fully quantify the role of the stent. The rectangular stent in the unsteady flow condition was observed to be optimal and decreased the magnitude of velocity in an aneurysm neck. The reduction or enhancement rate of flow characteristics of a rectangular strut shape was effective to reduce the flow in an aneurysm, compared with other strut shape and non-stented model.

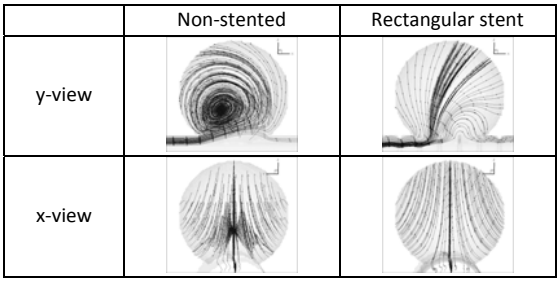

Figure 10, Streamline plot inside an aneruysm

By the small porosity and rectangular strut shape, it is possible to eliminate the strong vortex completely and to create a high viscosity region. An efficient stent should be designed so as to decrease the direct influence of the main flow. For a given porosity, the rectangular shape strut would seem preferable.

The results shown here already indicate that the current fluid solver based on the LBM is a very promising method for blood flow analysis, particularly when complicated geometries were used. More realistic artery geometry and blood models will be used in the future study.

References

1. G Geremia, M Haklic, L Brennecke, *AJNR* 15, 1223-31, 1994
2. BB Lieber, AP Stancampiano, AK Wakhloo, *Ann. Biomed. Eng*. 25, 460-469, 1997
3. F Turjman, TF Massoud, C Ji, G Guglielmi, F Vinuela, J Robert, *AJNR* 15, 1087-1090, 1994
4. JC Han, LR Glicksman, WM Rohsenow, *Int. J. Heat Mass Transf*. 21, 1143-1155, 1978
5. M Aenis, AP Stancampiano, AK Wakhloo, BB Lieber, ASME J Biomech Eng, 119, 206-212, 1997
6. SCM Yu, JB Zhao, Med Eng Phys, 21, 133-141. 1999
7. S Chen, GD Doolean, Ann Rev Fluid Mech, 30, 329-6, 1998
8. M Yoshino, Y Hotta, T Hirozane, E Endo, J non-Newtonian Fluids mech., 147, 69-78, 2007
9. RB Bird, RC Armstrong, o Hassager, Dynamics of Polymeric Liquids, Vol 1, Fluids Dynamics, 2nd Ed., John Wiley & Sons, New York, 1987
10. L.S. Luo, *Phys. Rev. E*. 62, 4982-4996, 2000
11. S Chen, D Martinez, R Mei, *Phys Fluids*, 8, 2527-36, 1996
12. M Hirabayashi, M Ohta, DA Rufunacht, B Chopard, Future Generation Computer Systems, 20, 925-934, 2004
13. Bruce R. Munson, Donald F. Young, Theodore H. Okiishi, *Fundamentals of Fluid Mechanics, 5th Edition* (2006)
14. YH Kim, JS Lee, Multiphase non-Newtonian effects on pulsatile hemodynamics in a coronary artery, Int J Num Meth Fluid, 2008, In press.